Please do not adjust margins

Journal Name

Article

Preparation and Characterisation of Heterobimetallic Copper---Tungsten Hydride Complexes

Received 00th January 20xx,
Accepted 00th January 20xx

DOI: 10.1039/x0xx00000x

www.rsc.org/

Alexandra Hicken[a,b], Andrew J. P. White[b], and Mark R. Crimmin[b]*

The preparation and structural characterisation of three new heterobimetallic hydride complexes containing 3-centre,2-electron W–H–Cu bonds is reported. These complexes have been characterised by single crystal X-ray crystallography and multinuclear NMR spectroscopy. The bonding in these complexes has been analysed by DFT calculations.

Introduction

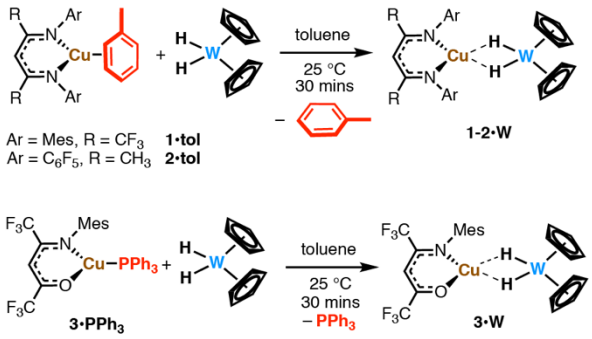
In the past few years, metal---metal cooperation has gained increasing attention as an innovative strategy in catalysis.[1-4] The co-existence of two or more metals in a single active site of a catalyst offers a means to control both activity and selectivity.[5-8] These studies have, in part, been inspired by metalloenzymes which often use more than one 1st row transition metal to achieve some remarkable chemical transformations. For example, the NiFe hydrogenase enzyme catalyses H^+ reduction and the microscopic reverse hydrogen splitting. Key intermediates in the catalytic cycle for this transformation are proposed to contain a 3-centre,2-electron Ni–H–Fe motif.[9]

In the past few years, we have pursued a research programme investigating the reactivity of complexes incorporating asymmetric 3-centre,2-electron M^1–H–M^2 bonds (M^1 = Zr, Cu, Rh, Ru, Pd; M^2 = Al, Zn, Mg, Ca, Au).[10-15] As part of these studies, we have documented the reversible coordination of M^2–H bonds to bent, two-coordinate, d^{10} β-diketiminate supported copper(I) fragments.[10,11,13,14] Based on a combination of X-ray diffraction, NMR spectroscopy and computational data, these complexes have been formulated as σ-complexes of copper(I). The 3-centre,2-electron M–H–Cu bond includes a large ionic contribution and can be considered as a donor–acceptor interaction. This contribution stems, primarily, from electron donation from the η^2-coordinated M^2–H bond into a low-lying unoccupied orbital on the {CuL_2} of largely 4s character. In related work we showed that four-coordinate boranes, BH_3•L (L = NMe_3, 2,6-lutidine), reversibly bind to the same copper(I) fragments by an $\eta^2;\eta^2$-coordination mode.[11,13] Both η^2- and $\eta^2;\eta^2$-coordination geometries have been rationalised by molecular orbital theory.

Herein we report the preparation and properties of a series of bis(σ-complexes) formed from the addition of tungsten dihydrides to bent d^{10} copper(I) fragments. These new species find rich precedent in the work of Caulton, Chaudret and others who have prepared related complexes of the coinage metals containing M^3–H–Cu, M^3–H–Ag, and M^3–H–Au linkages (M^3 = transition metal).[16-22]

Results and Discussion

The tungsten dihydride complex [(η^5-C_5H_5)$_2$$WH_2$] reacts with the copper(I) complexes **1-2•tol or 3•PPh_3** to give the corresponding bis(σ-complexes) **1-3•W** in 43 – 57% isolated yield (Scheme 1). These reactions occur with displacement of either the toluene or phosphine ligand from the copper(I) centre.



Scheme 1 - Preparation of heterobimetallic complexes **1-3•W**

[a] SSCP DTP, Grantham Institute, Imperial College London, South Kensington, London, SW7 2AZ, UK.
[b] Department of Chemistry, Imperial College London, South Kensington, London, SW7 2AZ, UK.

† Electronic Supplementary Information (ESI) available: Full details of the experiments, crystallographic data for **1-3•W** and calculations. See DOI: 10.1039/x0xx00000x

Please do not adjust margins

Journal Name

Article

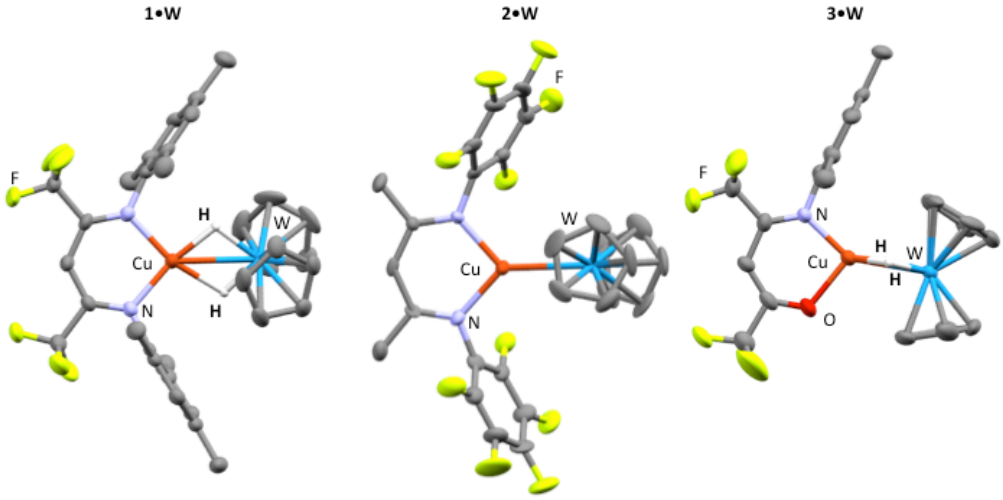
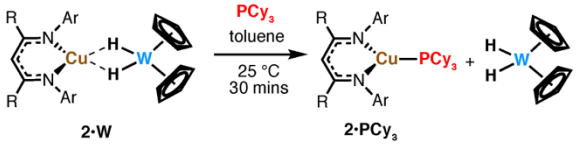


Figure 1 - X-ray structures of **1-3•W**, selected bond lengths (Å) and angles (°). **1•W**: Cu(1A)–W(1A) = 2.7369(6); Cu(1A)–H(1A)–W(1A) = 111.07(1.90); Cu(1A)–H(2A)–W(1A) = 104.15(2.48) . **2•W**: Cu(1)–W(1) = 2.7220(12); **3•W**: W(1)–Cu(1) = 2.6263(10).

Single crystals of **1-3•W** could be grown from toluene/*n*-heptane mixtures at −35 °C, and in the case of **1•W** and **3•W**, afforded data of high enough quality to locate the positions of the hydrides from the difference electron density map (Figure 1). The metal---metal distances in these complexes (**1•W**, 2.7369(6) Å; **2•W**, 2.7220(12) Å; **3•W**, 2.6263(10) Å) are beyond the sum of the radii defined by Pauling (2.47 Å) [23] and Pyykkö (2.49 Å).[24] For comparison, the Cu---W bond in [(η^5-C_5H_5)W(CO)$_2${Cu(PPh_3)$_2$)}] is 2.721(1) Å and is supported by semi-bridging carbonyl ligands.[25] The most striking structural distinction between complexes **1-3•W** lies in the torsion angle created by the plane containing the {CuL_2} fragments and the plane containing the {WH_2} moiety. In the solid state, this varies from planar to almost orthogonal, whereby these extremes represent square planar and tetrahedral geometries at Cu(I) respectively (**1•W**, 44°; **2•W**, 79°; **3•W**, 0°).

^{1}H and ^{19}F NMR spectra show a series of defined resonances for **1-3•W** in benzene-d_6 solution and no evidence for fragmentation in the copper and tungsten monometallic complexes was obtained at 298K. We have previously shown that related copper σ-complexes are weakly bound and are in equilibrium with the arene solvates in solution.[10,11,13,14] In benzene-d_6, a sharp singlet with characteristic tungsten satellites can be observed upfield in the ^{1}H NMR spectra (**1•W**; -12.4 ppm, **2•W**; -12.2 ppm, **3•W**; -13.5 ppm). A small increase in the $^1J_{W-H}$ coupling constants is recorded across the series (**W**; 72.0 Hz < **1•W**; 72.3 Hz < **2•W**; 75.7 Hz < **3•W**; 76.4 Hz). A comparison of the IR spectra of **W** with those measured for **1-3•W** confirmed that the W–H stretching frequencies could not be observed in the case of the heterobimetallic complexes.[26] It is likely these absorptions are shifted to the fingerprint region and overlap with those of the ligand systems.

Reaction of **2•W** with PCy_3 results in ligand exchange between [(η^5-C_5H_5)$_2WH_2$] and PCy_3, and was confirmed by independent *in-situ* synthesis of **2•PCy$_3$** (Scheme 2). Initial attempts to eliminate H_2 from these heterobimetallics has proven unsuccessful. Photolysis (400 W Hg lamp) led to no reaction and attempts to deprotonate **1•W** with $LiCH_2SiMe_3$ led to the crystallisation of an unusual lithium organocuprate which incorporates two coordinate tungsten dihydride moieties (see ESI for further details). DFT calculations suggest that H_2 elimination from these heterobimetallic complexes to form {L_2Cu–WCp_2} is significantly endergonic with ΔG°_{rxn} = +39 to +45 kcal mol^{-1}.



2·W 2·PCy$_3$

Scheme 2 –Reaction of **2•W** with PCy_3

Further experiments suggest that the hydrides of **2•W** do not undergo chemical exchange with external dihydrogen. The reaction of **2•W** with 1 atm. D_2 was followed by ^{1}H NMR spectroscopy. While at room temperature no exchange was observed, the use of elevated temperatures (80°) led to the slow decomposition of the complex **2•W** with no evidence for H/D exchange.

This journal is © The Royal Society of Chemistry 20xx

Please do not adjust margins

The structure and bonding of **1-3•W** have been scrutinised by calculations. DFT calculations using the solid-state structures as an input gave geometries that are in good agreement with experimental data.[27] These data confirmed the position of the hydride atoms and all in cases the $\eta^2;\eta^2$-coordination mode. In line with the previous findings, the analyses show that the dominant bonding in **1-3•W** is through the metal–hydride interactions rather than significant metal---metal interactions.

NBO calculations show that the σ-donation from the two W–H bonds to Cu is much greater than the components of the back-donation. The back-donation comprises of donation from a filled copper d-orbitals to the two σ*W–H orbitals and a low-lying vacant d-orbital of the tungstenocene dihydride moiety.[28] The latter component signifies a weak metal---metal interaction. Both Wiberg bond indices and second-order perturbation analysis suggest that the weak metal---metal interaction in **3•W** is the most significant of the series and is greater than **1-2•W** (Figure 2). In order to benchmark, and qualify, the amount of back-donation observed in **1-3•W** further NBO calculations were performed on the copper ethylene adducts **1-3•C_2H_4**.[29] Significantly more back-donation is observed in the case of **1-3•C_2H_4**.

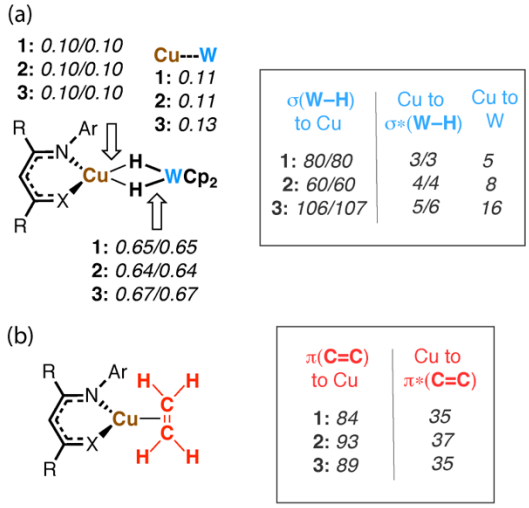


Figure 2 – Selected bonding metrics on **1-3•W** obtained from DFT calculations. a) Wiberg bond indices and data from second order perturbation analysis of **1-3•W**. b) data from second order perturbation analysis of **1-3•C_2H_4**, values in kcal mol^{-1}.

QTAIM calculations reveal that even though the metal---metal interaction across **1-3•W** is indeed weak, bond critical paths between Cu and W can be seen in the case of **1•W** and **3•W** (Figure 4).

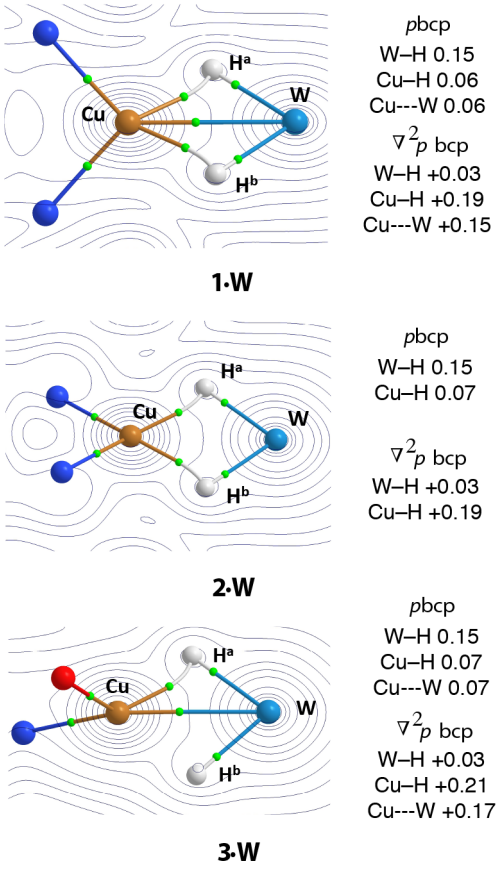


Figure 3 – QTAIM calculations on **1-3•W**.

The acuteness of H–M–H angle of metallocene complexes has been used as a crude metric to assess the possibility of metal---metal interactions in donor–acceptor complexes. A more obtuse H–M–H angle may indicate increased metal---metal interaction. For example, Bergman and co-workers have shown that upon coordination of Ph_3Al to $[Cp^*Ir(PMe_3)(H)_2]$ the H–Ir–H angle widens by 20°.[30] This result has been interpreted as evidence for metal–metal bonding in the adduct $[Cp^*Ir(PMe_3)(H)_2(AlPh_3)]$. Consistent with the NBO and QTAIM analysis, the calculated structures reveal a small increase in the H–W–H bond angle across the series (**1•W** ~ **2•W** < **3•W**), suggesting a more significant Cu---W interaction in the latter (**1•W**; 81.7°, **2•W**; 81.2°, **3•W**; 84.3°).

The presence of weak M---M' bond character in **1•W** and **3•W** is in contrast to similar complexes containing a three-centre,two-electron M–H–M' interactions. Sadighi and co-workers concluded that a symmetrical, cationic complex containing a $\{Cu–H–Cu\}^+$ moiety is characterised by an open three-centre interaction. In this instance, the only metal---metal interaction occurs through the bridging hydride.[31] Our own investigations into neutral complexes containing asymmetric {Au–H–Cu} groups have led to similar conclusions, with the main difference to the $\{Cu–H–Cu\}^+$ analogue being the asymmetry of the electron density in the three-centre core.[14] Furthermore, QTAIM analysis on related main group adducts in which $[(\eta^5\text{-}C_5H_5)_2WH_2]$ is coordinated to either BF_3 or $AlMe_3$

This journal is © The Royal Society of Chemistry 20xx

Please do not adjust margins

Please do not adjust margins

indicates that no bond critical point is observed between the two metals.[32]

Further bonding analysis provides an explanation for the structural variation in the single crystal diffraction studies of **1-3•W**. While borane adducts of these copper fragments have, to date, demonstrated solid state structures that are strictly tetrahedral at copper, the tungsten analogues appear to adopt a variety of geometries between the extremes of tetrahedral and square planar in the solid state. The lack of a geometric preference can be understood by inspecting the frontier molecular orbitals (fMOs) of the {CuL_2} fragment and considering them in combination with the NBO analysis. The dominant bonding interaction involves donation into an orbital that is largely 4s-based and approximately spherically symmetric. This interaction will be retained regardless of the torsion angle between the two metal fragments. Moreover, back-donation from copper to the tungsten fragment, while weak, is possible from two orthogonal filled orbitals on the {CuL_2} fragment and as such is possible in both square planar and tetrahedral geometries (Figure 4).

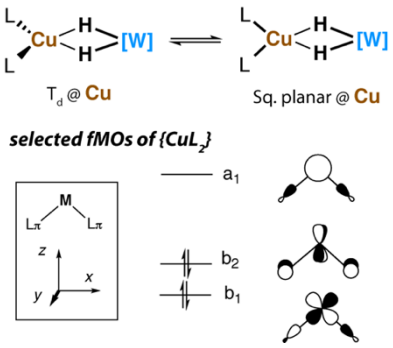


Figure 4 – Comparison of tetrahedral and square planar geometries at copper(I)

Single-point calculations in which a N–Cu---W–C torsion angle was varied incrementally from +90° to -90° were performed on **1•W**. These calculations show that the difference between the minimum and maximum energy on the potential energy surface is only ΔE(SCF) = +19 kcal mol^{-1}. Hence, the interconversion of tetrahedral and square planar geometries at copper should be facile. The preference for the observed solid state conformers of **1-3•W** is likely a result of weak secondary interactions in the coordination sphere and crystal packing effects (Figure 3). Similar calculations on related copper(I) bis(σ-borane) complexes show that the square planar geometry is in fact a transition state, but that interconversion of the isomers is equally, if not more, facile with ΔE(SCF) = 5 kcal mol^{-1}.[13]

Conclusions

In summary, we report the preparation and characterisation of three new heterobimetallic hydride complexes containing Cu–H–W bonds. In all cases an $\eta^2;\eta^2$-coordination mode is observed with the tungsten dihydride acting as a chelating ligand for copper(I). Multinuclear NMR spectroscopy data are consistent with these complexes being robust under ambient conditions in solution, although ligand exchange, likely by a dissociative mechanism, can be observed upon addition of an external phosphine ligand. Computational analysis of the bonding shows that the dominant interaction in the W–H–Cu 3-centre,2-electron core can be found between the tungsten and hydride atoms with weaker bonds between the copper and hydride atoms and the two metals. The calculations, in combination with solid state structures suggest that the interconversion between tetrahedral and square planar geometries at copper(I) is facile.

Experimental

General Experimental Procedures

All manipulations were carried out using standard Schlenk-line and glovebox techniques under an inert atmosphere of argon or dinitogen. A MBraun Labmaster glovebox was employed, operating at < 0.1 ppm O_2 and < 0.1 ppm H_2O. Solvents were dried over activated alumina from an SPS (solvent purification system) based upon the Grubbs design and degassed before use. Glassware was dried for 12 h at 120 °C prior to use. Benzene-d_6 and toluene-d_8 were stored over 3Å molecular sieves and distilled prior to use. NMR-scale reactions were conducted in J. Youngs tap tubes and prepared in a glovebox. All heating mentioned was done using silicone oil baths. ^1H, ^{19}F and ^{13}C, NMR spectra were obtained on BRUKER 400 MHz or 500 MHz machines unless otherwise stated; all peak intensities are derived internal standard peak with values quoted in ppm. Data was processed using the MestReNova or Topspin software. PCy_3, [(η^5-$C_5H_5)_2WH_2$] and $LiMe_2CH_3$ were purchased from Sigma Aldrich. **1-2•tol** and **3•PPh$_3$** were prepared according to known literature procedures.[13] D_2 99.95% atom D was purchased from sigma Aldrich and passed through an Agilent oxygen/moisture trap before use.

1•W

In a glove box, **1$_2$•tol** (61 mg, 0.055 mmol, 1 equiv.) was weighed into a vial and dissolved in toluene (1.5 mL). Similarly, [(η^5-$C_5H_5)_2WH_2$] (38 mg, 0.11 mmol, 2 equiv.) was weighed and dissolved in toluene (1.5 mL). The solution containing [(η^5-$C_5H_5)_2WH_2$] was added dropwise over 5 minutes to the stirred solution of **1$_2$•tol**. The reaction mixture was stirred for 30 minutes at 25 °C. The red solution was filtered using a glass fibre and the concentrated *in vacuo* to ½ of its original volume before *n*-heptane (1.5 mL) was added. The reaction mixture was left at -35 °C overnight to give dark red crystals of 1•W (46 mg, 0.05 mmol, 49 %). ^1H NMR (C_6D_6, 298 K, 500 MHz) δ -12.4 (s, 2H, $^1J_{W-H}$ = 73.6 Hz, W–(H)$_2$–Cu), 2.17 (s, 6H, Ar–Me_{Cu}), 2.32 (s, 12H, Ar–Me_{Cu}), 3.65 (s, 10H, Cp_W), 6.26 (s, 1H, CH_{Cu}), 6.81 (s,

This journal is © The Royal Society of Chemistry 20xx

Please do not adjust margins

Please do not adjust margins

4H, Ar–H_{Cu}); $^{13}C\{^1H\}$ NMR (C_6D_6, 298 K, 125 MHz) δ 19.2, 21.0, 22.2, 74.3, 83.6 (sept, $^3J_{C-F}$ = 5.4 Hz), 122.7 (q, $^1J_{C-F}$ = 288.3 Hz), 129.0, 130.4, 132.6, 147.2, 151.7 (q, $^2J_{C-F}$ = 24.2 Hz); ^{19}F NMR (C_6D_6, 298 K, 470.4 MHz) δ -64.0. Elemental analysis calc. for $C_{33}H_{35}CuF_6N_2W$: C, 48.28; H, 4.30; N, 3.41. Found: C, 48.39; H, 4.20; N, 3.54.

2•W

In a glove box, **2•tol** (62 mg, 0.11 mmol, 1 equiv.) was weighed into a vial and dissolved in toluene (1.5 mL). Similarly, [(η^5-C_5H_5)$_2$$WH_2$] (38 mg, 0.11 mmol, 1 equiv.) was weighed and dissolved in toluene (1.5 mL). The solution containing [(η^5-C_5H_5)$_2$$WH_2$] was added dropwise over 5 minutes to the stirred solution of **2•tol**. The reaction mixture was stirred for 30 minutes at 25 °C. The orange solution was filtered using a glass fibre and the concentrated *in vacuo* to ½ of its original volume before *n*-heptane (1.5 mL) was added. The reaction mixture was left at -35 °C overnight to give yellow crystals of 2•W (64 mg, 0.08 mmol, 69 %). ^1H NMR (C_6D_6, 298 K, 500 MHz) δ -12.2 (s, 2H, $^1J_{W-H}$ = 72.2 Hz, W–(H)$_2$–Cu), 1.73 (s, 6H, Ar–Me_{Cu}), 3.76 (s, 10H, Cp_W), 4.98 (s, 1H, CH_{Cu}); $^{13}C\{^1H\}$ NMR (C_6D_6, 298 K, 125 MHz) δ 23.8, 73.6, 97.6, 129.5 (m), 135.7 (m), 138.3 (m), 141.5 (m), 165.4; ^{19}F NMR (C_6D_6, 470.4 MHz, 298 K) δ -166.2 (m, 2F), -165.2 (m, 4F), -150.8 (m, 4F). Elemental analysis calc. for $C_{27}H_{19}CuF_{10}N_2W$: C, 40.09; H, 2.37; N, 3.46. Found: C, 40.20; H, 2.35; N, 3.56.

3•W

In a glove box, **3•PPh$_3$** (67.7 mg, 0.11 mmol, 1 equiv.) was weighed into a vial and dissolved in toluene (1.5 mL). Similarly, [(η^5-C_5H_5)$_2$$WH_2$] (38 mg, 0.11 mmol, 1 equiv.) was weighed and dissolved in toluene (1.5 mL). The solution containing [(η^5-C_5H_5)$_2$$WH_2$] was added dropwise over 5 minutes to the stirred solution of **3•PPh$_3$**. The reaction mixture was stirred for 30 minutes at room temperature. The red solution was filtered using a glass fibre and the solvent removed *in vacuo* to give the crude as an orange solid. The crude was triturated with n-hexane (3 mL) giving **3•W** as a red crystalline solid (39 mg, 0.05 mmol, 48 %). ^1H NMR (C_6D_6, 298 K, 500 MHz) δ -13.5 (s, 2H, $^1J_{W-H}$ = 76.4 Hz, W–(H)$_2$–Cu), 2.07 (s, 3H, Ar–Me_{Cu}), 2.19 (s, 6H, Ar–Me_{Cu}), 3.99 (s, 10H, Cp_W), 6.20 (s, 1H, CH_{Cu}), 6.69 (s, 2H, Ar–H_{Cu}); $^{13}C\{^1H\}$ NMR (C_6D_6, 298 K, 125 MHz) δ 18.8, 20.9, 75.6, 85.4, 120.5 (q, $^1J_{C-F}$ = 286.6 Hz), 120.5 (q, $^1J_{C-F}$ = 288.4 Hz), 128.4, 128.8, 133.4, 145.6, 155.1 (q, $^2J_{C-F}$ = 26.2 Hz), 170.3 (q, $^2J_{C-F}$ = 30.9 Hz); ^{19}F NMR (C_6D_6, 298 K, 470.4 MHz) δ -74.7 (3F), -65.9 (3F). Elemental analysis calc. for $C_{26}H_{30}CuF_6NOW$: C, 40.96; H, 3.44; N, 1.99. Found: C, 40.77; H, 3.52; N, 2.05.

Ligand Exchange

In a glovebox, **2•W** (6 mg, 0.007 mmol) was dissolved in C_6D_6 (500 µL) and transferred to an NMR tube with J Youngs adapter. Similarly, **PCy$_3$** (2 mg, 0.007 mmol) was dissolved in C_6D_6 (100 µL) and added to the tube containing the copper complex. The reaction was followed *via* ^1H, ^{19}F and ^{31}P NMR spectroscopy whereby **2•PCy$_3$** and [(η^5-C_5H_5)$_2$$WH_2$] were observed *in-situ*. The presence of **2•PCy$_3$** was confirmed by independent *in-situ* characterisation *via* reaction of one equivalent of **2•tol** and **PCy$_3$**. ^1H NMR (C_6D_6, 298 K, 400 MHz) δ 1.28 (m, 33H), 1.64 (s, 6H), 5.01 (s, 1H); ^{19}F NMR (C_6D_6, 298 K, 376.5 MHz) δ -149.9 (m, 4F), -164.4 (m, 4F), -165.5 (m, 4F); $^{31}P\{^1H\}$ NMR (C_6D_6, 298 K, 162.0 MHz) δ 20.8 (s).

H/D Exchange

In a glovebox, **2•W** (19 mg, 0.023 mmol) was dissolved in C_6D_6 (600 µL) and transferred to an NMR tube with J Youngs adapter. The tube was freeze-pump thawed on a Schlenk line three times before being exposed to an atmosphere of D_2. The reaction was followed *via* ^1H NMR spectroscopy. No H/D exchange was observed before the onset of decomposition of **2•W** at 80 °C.

Conflicts of interest

There are no conflicts to declare.

Acknowledgements

We are grateful to the Royal Society for provision of a University Research Fellowship (MRC) and to the Leverhulme Trust (RPG-2015-248) for generous funding. We also thank the Science and Solutions for a Changing Planet Doctoral Training Program for provision of a National Environmental Research Council funded PhD studentship (AH). Dr. Bryan Ward is thanked for help with the DFT calculations.

Associated Content

Electronic versions of the NMR spectra as as .mnova and .mnpub files along with coordinates for the optimized DFT structures are available at DOI:10.14469/hpc/4078.

Notes and references

1 I. G. Powers and C. Uyeda, *ACS Catal.*, 2017, **7**, 936–958.
2 N. P. Mankad, *Chem. Eur. J.*, 2016, **22**, 5822–5829.
3 B. G. Cooper, J. W. Napoline and C. M. Thomas, *Cat. Rev.*, 2012, **54**, 1–40.
4 M. J. Butler and M. R. Crimmin, *Chem. Comm.*, 2017, **53**, 1348–1365.
5 S. Bagherzadeh and N. P. Mankad, *J. Am. Chem. Soc.*, 2015, **137**, 10898–10901.
6 M. K. Karunananda and N. P. Mankad, *J. Am. Chem. Soc.*, 2015, **137**, 14598–14601.
7 B. Wu, K. M. Gramigna, M. W. Bezpalko, B. M. Foxman and C. M. Thomas, *Inorg. Chem.*, 2015, **54**, 10909–10917.
8 R. C. Cammarota, M. V. Vollmer, J. Xie, J. Ye, J. C. Linehan, S. A. Burgess, A. M. Appel, L. Gagliardi and C. C. Lu, *J. Am. Chem. Soc.*, 2017, **139**, 14244–14250.
9 D. Brazzolotto, M. Gennari, N. Queyriaux, T. R. Simmons, J. Pécaut, S. Demeshko, F. Meyer, M. Orio, V. Artero and C. Duboc, *Nat. Chem.*, 2016, **8**,

Please do not adjust margins

Please do not adjust margins

1054–1060.
10 A. E. Nako, Q. W. Tan, A. J. P. White and M. R. Crimmin, *Organometallics*, 2014, **33**, 2685–2688.
11 A. E. Nako, A. J. P. White and M. R. Crimmin, *Dalton Trans.*, 2015, **44**, 12530–12534.
12 O. Ekkert, A. J. P. White and M. R. Crimmin, *Angew. Chem. Int. Ed.*, 2016, **55**, 16031–16034.
13 A. Hicken, A. J. P. White and M. R. Crimmin, *Inorg. Chem.*, 2017, **56**, 8669–8682.
14 A. Hicken, A. J. P. White and M. R. Crimmin, *Angew. Chem. Int. Ed.*, 2017, **56**, 15127–15130.
15 M. J. Butler, A. J. P. White and M. R. Crimmin, *Angew. Chem. Int. Ed.*, 2016, **55**, 6951–6953.
16 L. F. Rhodes, J. C. Huffman and K. G. Caulton, *J. Am. Chem. Soc.*, 1984, **106**, 6874–6876.
17 A. Antiñolo, F. Carrillo, B. Chaudret, M. Fajardo, J. Fernández-Baeza, M. Lanfranchi, H.-H. Limbach, M. Maurer, A. Otero and M. A. Pellinghelli, *Inorg. Chem.*, 1994, **33**, 5163–5164.
18 L. F. Rhodes, J. C. Huffman and K. G. Caulton, *J. Am. Chem. Soc.*, 1983, **105**, 5137–5138.
19 T. Arliguie, B. Chaudret, F. A. Jalon, A. Otero, J. A. Lopez and F. J. Lahoz, *Organometallics*, 1991, **10**, 3411–3411.
20 A. Antiñolo, F. Carrillo-Hermosilla, B. Chaudret, M. Fajardo, J. Fernández-Baeza, M. Lanfranchi, H.-H. Limbach, M. Maurer, A. Otero and M. A. Pellinghelli, *Inorg. Chem.*, 1996, **35**, 7873–7881.
21 A. Albinati, F. Demartin, L. M. Venanzi and M. K. Wolfer, *Angew. Chem. Int. Ed.*, 1988, **27**, 563–563.
22 A. Albinati, H. Lehner, L. M. Venanzi and M. Wolfer, *Inorg. Chem.*, 1987, **26**, 3933–3939.
23 L. Pauling, *J. Am. Chem. Soc.*, 1947, **69**, 542–553.
24 P. Pyykkö and M. Atsumi, *Chem. Eur. J.*, 2009, **15**, 186–197.
25 L. Carlton, W. E. Lindsell, K. J. McCullough and P. N. Preston, *J. Chem. Soc., Dalton Trans.*, 1984, **0**, 1693–1701.
26. Infrared data recorded on **W•Al(CH$_3$)$_3$** a trimethylaluminium adduct were reported to occur at the same wavelengths as the parent dihydride **W**. A. Storr, B. S. Thomas, *Can. J. Chem.* **1971**, *49*, 2504–2507
27. These calculations were performed using the B3PW91 functional with GD3BJ dispersion and hybrid basis set SDDAll (Cu, W), 6-311G* (others). For further information on methodology see supporting information section 3.
28. These values represent selected data regarding interactions between the lowest energy orbitals on copper, however other significant contributions to higher energy orbitals exist.
29 X. Dai and T. H. Warren, *J. Am. Chem. Soc.*, 2004, **126**, 10085–10094.
30 Jeffery T Golden, Thomas H Peterson, Patrick L Holland, A. Robert G Bergman and R. A. Andersen, *J. Am. Chem. Soc.*, 1998, **120**, 223–224.
31 C. M. Wyss, B. K. Tate, J. Bacsa, T. G. Gray and J. P. Sadighi, *Angew. Chem. Int. Ed.*, 2013, **52**, 12920–12923.
32 M. Amati and F. Lelj, *Can. J. Chem.*, 2009, **87**, 1406–1414.

 This journal is © The Royal Society of Chemistry 20xx

Please do not adjust margins